ACADEMIC PRESS

Available online at www.sciencedirect.com
SCIENCE DIRECT®

Journal of Catalysis 218 (2003) 427–437

JOURNAL OF CATALYSIS

www.elsevier.com/locate/jcat

Mechanisms of *n*-decane hydrocracking on a sulfided NiW on silica-alumina catalyst

Martial Roussel,[a] Jean-Louis Lemberton,[a,*] Michel Guisnet,[a] Tivadar Cseri,[b] and Eric Benazzi[b]

[a] *Laboratoire de Catalyse en Chimie Organique, Université de Poitiers, 40 avenue du Recteur Pineau, 86022 Poitiers cedex, France*
[b] *Institut Français du Pétrole, Kinetics and Catalysis Division, 1&4 avenue de Bois-Préau, 92852 Rueil-Malmaison cedex, France*

Received 13 January 2003; revised 28 March 2003; accepted 2 April 2003

Abstract

The hydrocracking of *n*-decane was carried out on a sulfided NiW/silica-alumina catalyst and for comparison on a sulfided NiW/USHY zeolite catalyst (fixed-bed reactor, 380 °C, 6 MPa total pressure, presence of sulfur and nitrogen-containing compounds in the feed). As could be expected from the weak acidity of the silica-alumina support, hence from the high ratio between the hydrogenating and the acid functions, at high *n*-decane conversion NiW/silica-alumina was found more selective than NiW/zeolite for the formation of isomerization products. The difference in selectivity between the two catalysts was even more significant at low *n*-decane conversion, due to a direct cracking of *n*-decane which occurred on NiW/silica-alumina in addition to the classical bifunctional process. This reaction was shown to take place on the sulfided NiW phase, possibly through abstraction of a proton of the molecule by a basic surface sulfur atom.

Keywords: Hydrocracking; Bifunctional catalysts; NiW sulfides; Silica-alumina; USHY zeolite; *n*-Decane

1. Introduction

High-pressure hydrocracking is a catalytic refining process allowing an upgrade of rather heavy petroleum fractions such as vacuum distillates into gasoline or middle distillates, kerosene, and gas oil [1–4]. It is also used to upgrade some products obtained from other processes, such as deasphalted oils and cycle oils from fluid catalytic cracking [1,5]. A major interest of hydrocracking is its great versatility since it is possible to equilibrate supply (gasoline or middle distillates) and demand. The growing demand for middle distillates, which cannot be obtained using fluid catalytic cracking, makes hydrocracking a strategic process in a modern refinery [2,6,7].

Moreover, in addition to the cracking of the molecules, the hydrocracking process ensures the elimination of sulfur- and nitrogen-containing compounds as well as a deep saturation of aromatics. This allows the production of high-quality fuels which will match the future and more stringent specifications [1,8].

Hydrocracking catalysts are bifunctional, associating a hydro-dehydrogenating function with an acidic one. Since the feeds to be treated contain significant amounts of heteroatoms (sulfur and nitrogen), the catalysts must resist poisoning by hydrogen sulfide and ammonia. That is why the hydro-dehydrogenating function of industrial hydrocracking catalysts is generally provided by mixed sulfides of group VI and VIII metals, such as molybdenum or tungstene promoted by nickel or cobalt.

If gasoline is the required product, the acidic component of the catalyst will be preferably a zeolite, the strong acidity of which will favor successive cracking reactions of the feed molecules with formation of the desired light products [9]. On the contrary, the catalysts which would allow an optimal gas oil yield which would possess a moderate acidity, halfway between that of zeolites (low selectivity) and that of aluminas (too low activity). Amorphous supports like silica-aluminas could have such an acid strength [2,10–12].

Our objective was to study hydrocracking catalysts allowing a selective transformation of vacuum distillates into gas oil. For the reasons explained above, a sulfided NiW/silica-

* Corresponding author.
E-mail address: jean.louis.lemberton@univ-poitiers.fr (J.-L. Lemberton).

0021-9517/03/$ – see front matter
doi:10.1016/S0021-9517(03)00164-7

alumina catalyst was chosen, and was compared to a strongly acidic NiW/USHY zeolite catalyst. The model reaction used was the hydrocracking of *n*-decane, under conditions similar to the industrial ones: fixed-bed dynamic reactor, high hydrogen pressure, presence in the feed of sulfur- and nitrogen-containing compounds. In this work the nature and the repartition of the reaction products were examined and the reaction scheme established. The different selectivities were measured, in particular the isomerization/cracking selectivity which can be considered as representative of the selectivity of the catalyst for the production of middle distillates. To obtain a better understanding of the behavior of the NiW/silica-alumina catalyst, we also studied the transformation of *n*-decane on a nonacidic NiW/alumina catalyst, on an unpromoted W/silica-alumina catalyst, and finally on NiW/silica-alumina in the absence of nitrogen-containing compound in the feed.

2. Experimental

n-Decane hydrocracking was carried out in a flow reactor at 380 °C under a 6 MPa total pressure, with a hydrogen/*n*-decane molar ratio equal to 20. Dimethyl disulfide and aniline were added to *n*-decane in order to generate H_2S ($pH_2S = 6.1$ kPa) and NH_3 ($pNH_3 = 5$ kPa), respectively. The catalysts were first sulfided in the reactor by a *n*-heptane/dimethyl disulfide/aniline mixture, under the same pressures as those used for the *n*-decane hydrocracking reaction, and at a 0.27-min contact time (1/WHSV). The sulfiding feed was injected starting at 150 °C, and then the temperature was raised at 285 °C (1-h stage), 350 °C (2-h stage), and finally to 380 °C (reaction temperature). After about 2 h at 380 °C, the catalyst exhibited a stable activity for *n*-heptane hydrocracking. The sulfiding feed was then replaced by the reaction one: *n*-decane/dimethyl disulfide/aniline. Once a steady-state activity was reached, the contact time was changed by modifying the feed flow rate in order to obtain different conversion values. At the end of the *n*-decane hydrocracking experiment, the sulfiding feed was injected again under the same conditions as those used during sulfidation in order to check whether the catalyst deactivated or not during *n*-decane hydrocracking. No deactivation was observed with any of the catalysts used in the present work.

All the reaction products were analyzed on-line by gas-liquid chromatography (Varian 3400) on a 50 m CP-Sil5 capillary column (Chrompack), hydrogen being the carrier gas (15 psi), with a temperature programming from 45 to 85 °C (10 °C min^{-1}).

The NiW/silica-alumina catalyst contained 2.4 wt% Ni and 18.3 wt% W, which corresponds to a Ni/(Ni + W) molar ratio equal to 0.3. The amorphous silica-alumina support was obtained from Condea and contained 40 wt% silica and 60 wt% alumina. The specific surface area was 317 $m^2 g^{-1}$ and the pore volume 0.81 $cm^3 g^{-1}$.

Three other catalysts were used:

- NiW/zeolite, which is in fact a mixture of a USHY zeolite (20 wt%) with an alumina on which Ni and W were deposited. The framework Si/Al ratio of the USHY zeolite was about 15. The NiW/zeolite catalyst contained the same Ni and W amounts as the NiW/silica-alumina catalyst.
- NiW/alumina, containing the same Ni and W amounts as the NiW/silica-alumina catalyst. The alumina support (surface area 258 $m^2 g^{-1}$, pore volume 0.50 $cm^3 g^{-1}$) was obtained from Condea.
- W/silica-alumina, with the same W amount and the same silica-alumina support as the NiW/silica-alumina catalyst.

All the catalysts were prepared at the Institut Français du Pétrole in the form of extrudates (2 × 6 mm).

The acidities of the silica-alumina and alumina supports and of the pure USHY zeolite were determined by pyridine adsorption followed by FTIR spectroscopy (Nicolet Magna IR 550 spectrometer). The samples were first activated under dry air flow (60 ml min^{-1}) at 450 °C for 12 h and then under vacuum (10^{-5} mbar) at 200 °C for 1 h. Before pyridine adsorption, IR spectra were recorded at room temperature between 1300 and 3800 cm^{-1} in order to observe the OH groups. Pyridine was adsorbed on the sample at 150 °C. The IR spectra were recorded after pyridine desorption under vacuum (10^{-5} mbar) at different temperatures ranging from 150 to 550 °C. The number of the protonic sites was estimated by using the extinction coefficient for pyridinium ions (band at 1540 cm^{-1}) determined in a previous work [13].

3. Results

3.1. Acidity of the supports

Silica-alumina possessed only one type of terminal OH groups, already observed by Knözinger and colleagues [14]. On the contrary, several OH groups were observed on the USHY zeolite [13]: terminal OH groups, similar to those observed on silica-alumina, bridging OH in large cavities or in small cavities, and OH interacting with extraframework aluminum species. Five OH bands were observed on alumina [15]: OH coordinated to octahedral or to tetrahedral Al, and OH bridging tetrahedral and octahedral Al, and OH coordinated to 2 or to 3 octahedral Al.

Fig. 1 presents the number of Brønsted acid sites (μmol g^{-1}) measured on the silica-alumina support and on the pure USHY zeolite as a function of pyridine desorption temperature. The alumina support exhibited no Brønsted acidity.

The total number of Brønsted acid sites, measured by the amount of pyridine adsorbed at 150 °C, was much more significant on zeolite (784 μmol g^{-1}) than on silica-alumina

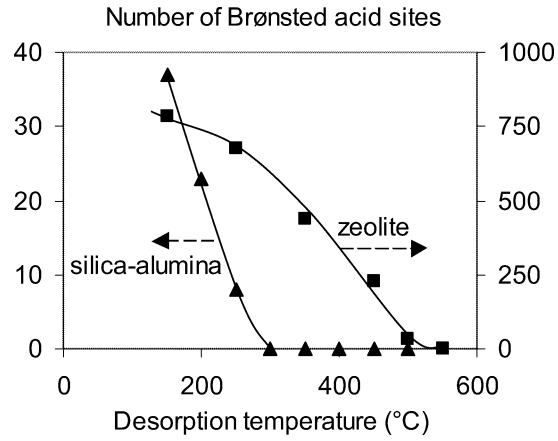

Fig. 1. Number of Brønsted acid sites (μmol g^{-1}) on the silica-alumina support and on the pure USHY zeolite as a function of pyridine desorption temperature (°C).

(37 μmol g^{-1}). Thus, the Brønsted acid sites were about 4 times more numerous on the alumina-zeolite support (which contained only 20 wt% zeolite) than on the silica-alumina support. Moreover, the Brønsted acid sites were much stronger on zeolite than on silica-alumina: pyridine was retained up to 500 °C on the zeolite, while it was no more detected on silica-alumina at 300 °C.

3.2. Hydrocracking of *n*-decane on NiW/silica-alumina

n-Decane transformed on NiW/silica-alumina into isomerization products I (monobranched isomers M and multibranched isomers B) and into cracking products C. Fig. 2 shows that M were the main reaction products, B and C being formed in much smaller amounts. B were secondary products, while M and C were directly formed, but the yield in C products increased at high *n*-decane conversions, which indicates the existence of a secondary cracking. The isomerization/cracking ratio (I/C) initially increased when the *n*-decane conversion increased and then decreased (Fig. 3). In the conversion range studied, this ratio was always very high (greater than 8), with a maximum value equal to 13 at a 20% *n*-decane conversion. The monobranched isomers/multibranched isomers ratio (M/B) decreased when the conversion of *n*-decane increased (Fig. 3) but remained very high, about 10 at a 30% *n*-decane conversion.

Table 1 presents the distribution of the monobranched isomers at a 25% conversion of *n*-decane, at a 0% conversion (extrapolated values) and at the thermodynamic equilibrium [16]. These isomers were methylnonanes (mC_9) and ethyloctanes (etC_8); propylheptane (prC_7) was not observed. The distribution depended on the conversion of *n*-decane, especially for 3-methylnonane ($3mC_9$) and 4-ethyloctane ($4etC_8$). This distribution was somewhat different from the distribution at the thermodynamic equilibrium, in particular at a zero conversion. However, the evolution of the distribution when the conversion of *n*-decane increased was that

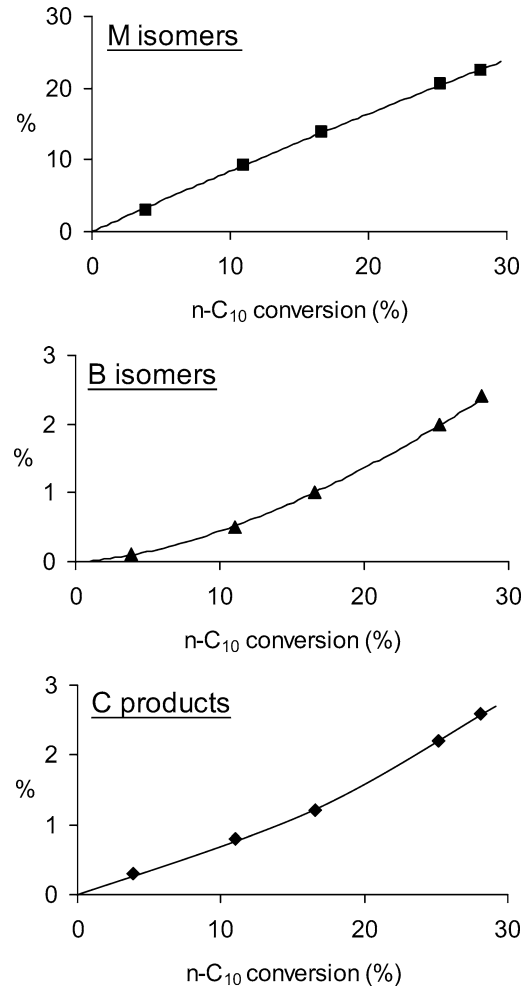

Fig. 2. Transformation of *n*-decane on NiW/silica-alumina: yields in the monobranched isomers M, in the multibranched isomers B, and in the cracking products C.

expected, i.e., tending to that at the thermodynamic equilibrium.

The distribution of the multibranched isomers is presented in Table 2. The products formed were dimethyloctanes, mainly 2,5- and 3,5-dimethyloctanes ($25 + 35$ dmC_8, not separated in the chromatographic analyses), 2,4-, 2,6-, 3,4-, and 4,5-dimethyloctanes ($24dmC_8$, $26dmC_8$, $34dmC_8$, and $45dmC_8$). 3-Methyl 4-ethylheptane ($3m4etC_7$) and a small amount of 3,4,5-trimethylheptane ($345tmC_7$) were also formed, while 2,3-dimethyloctane was not observed. The distribution of the multibranched isomers hardly depended on the conversion of *n*-decane and was rather different from the distribution at the thermodynamic equilibrium.

The cracking products were C_2 to C_8 molecules. All the methane produced was shown to result from dimethyl disulfide decomposition. Furthermore nonanes were not observed, which confirmed that cracking of *n*-decane into C_1 and C_9 did not occur. The distribution of the cracking products depended on the conversion of *n*-decane (Fig. 4). Under a 5% conversion, all the products were formed in similar molar amounts, except C_7 (mainly *n*-heptane) formed in larger

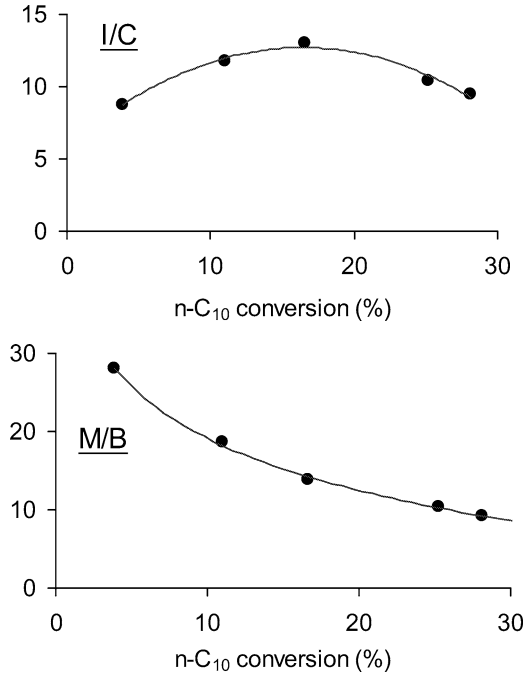

Fig. 3. Transformation of *n*-decane on NiW/silica-alumina: isomerization/cracking ratio I/C and monobranched isomers/multibranched isomers ratio M/B. Isomerization and cracking values are wt%.

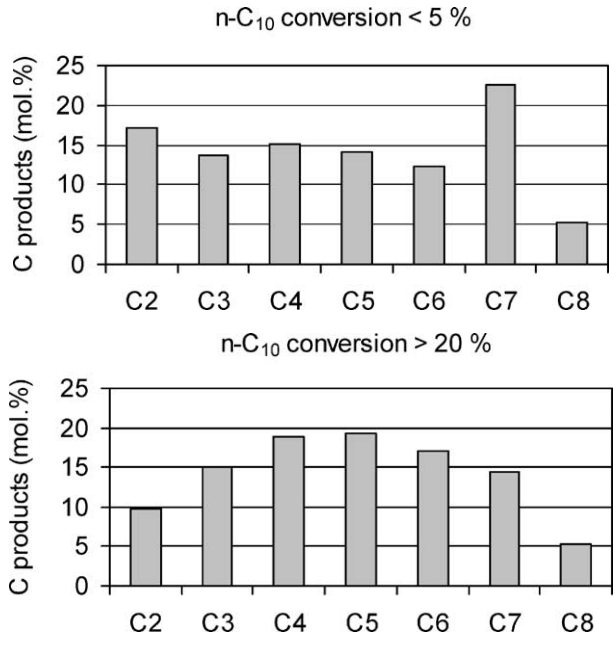

Fig. 4. Transformation of *n*-decane on NiW/silica-alumina: distribution (mol%) of the cracking products as a function of *n*-decane conversion.

Table 1
Distribution (mol%) of the monobranched isomers formed on NiW/silica-alumina at a zero conversion of *n*-decane (extrapolated values), at a 25% conversion, and at the thermodynamic equilibrium [16]

	$2mC_9$	$3mC_9$	$4mC_9$	$5mC_9$	$3etC_8$	$4etC_8$	$4prC_7$
$X(n\text{-}C_{10}) = 0$	22	32	27	11	4	4	0
$X(n\text{-}C_{10}) = 25$	22	27	25	11	5	10	0
TE	23.8	21.6	23.0	11.7	6.2	12.0	1.7

$X(n\text{-}C_{10})$, *n*-decane conversion (%). TE, thermodynamic equilibrium.

amounts, and C_8 (*n*-octane only) formed in lower amounts. The C_2/C_8, C_3/C_7, and C_4/C_6 molar ratios were different from the unity. Above a 20% conversion, the distribution took a gaussian shape centered on the C_5 molecules. The C_3/C_7 and C_4/C_6 molar ratios were close to 1. On the other hand (Fig. 5) the linear cracking products (*n*) were always largely favored when compared to the branched products (iso), even if the iso/*n* ratio increased when the conversion of *n*-decane increased. In the case of C_8 cracking products, only *n*-octane was observed.

3.3. Hydrocracking of *n*-decane on other bifunctional catalysts

Fig. 6 shows the conversion of *n*-decane as a function of the contact time on the NiW/silica-alumina, NiW/zeolite, NiW/alumina, and W/silica-alumina catalysts. The most active catalyst was NiW/zeolite: its activity was 75×10^{-4} mol h^{-1} g^{-1}, while that of NiW/silica-alumina was only 5.5×10^{-4} mol h^{-1} g^{-1}. On the other hand, the unpromoted W/silica-alumina catalyst had exactly the same activity as NiW/silica-alumina. NiW/alumina was the less active catalyst (1.0×10^{-4} mol h^{-1} g^{-1}).

On NiW/zeolite (Fig. 7), the monobranched isomers M and the multibranched isomers B were primary reaction products, the cracking products C being secondary reaction products. Both B and C products were formed in much more significant amounts than on NiW/silica-alumina (Fig. 2).

M and C products were primary reaction products on W/silica-alumina (Fig. 7), as was the case on NiW/silica-alumina. However the amount of B products formed increased faster on W/silica-alumina than on NiW/silica-alumina when the conversion of *n*-decane increased.

Table 2
Distribution (mol%) of the multibranched isomers formed on NiW/silica-alumina at a zero conversion of *n*-decane (extrapolated values), at a 25% conversion, and at the thermodynamic equilibrium [16]

	25 + 35 dmC_8	26 dmC_8	24 dmC_8	34 dmC_8	27 dmC_8	36 dmC_8	44 dmC_8	45 dmC_8	22 dmC_8	33 dmC_8	23 dmC_8	3m4et C_7	345tm C_7
$X(n\text{-}C_{10}) = 0$	28	10	14	10	5	3	4	15	3	1	0	7	0
$X(n\text{-}C_{10}) = 25$	25	9	7	6	5	6	5	12	4	4	0	4	3
TE	16.6	9.7	7.0	6.0	6.9	6.5	8.4	5.3	8.3	9.0	9.5	4.1	2.7

$X(n\text{-}C_{10})$, *n*-decane conversion (%). TE, thermodynamic equilibrium.

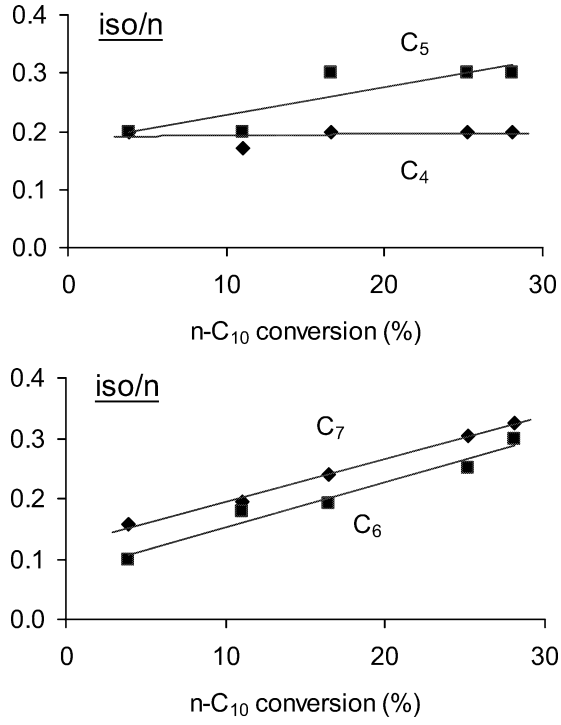

Fig. 5. Transformation of *n*-decane on NiW/silica-alumina: branched/linear ratio iso/*n* (mol%) of the cracking products.

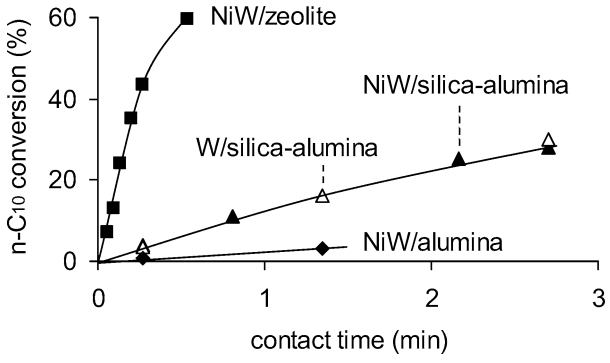

Fig. 6. Conversion of *n*-decane (%) on NiW/silica-alumina, NiW/zeolite, W/silica-alumina, and NiW/alumina.

B products were not observed with NiW/alumina. The most surprising result with such a nonacidic catalyst was that C products were formed in greater amounts than M products (Fig. 7).

Except at low *n*-decane conversion, the I/C ratio measured with NiW/zeolite was smaller than that measured with NiW/silica-alumina (Fig. 8). Moreover, the maximum observed with NiW/silica-alumina did not exist any more with NiW/zeolite: I/C regularly decreased when the conversion of *n*-decane increased. Due to the more significant amount of B products formed on NiW/zeolite, the M/B ratio was also smaller on this catalyst than on NiW/silica-alumina (Fig. 8).

The I/C ratio measured with W/silica-alumina initially increased when the conversion of *n*-decane increased (Fig. 8), as was the case with NiW/silica-alumina. However, no maximum was observed, at least in the range

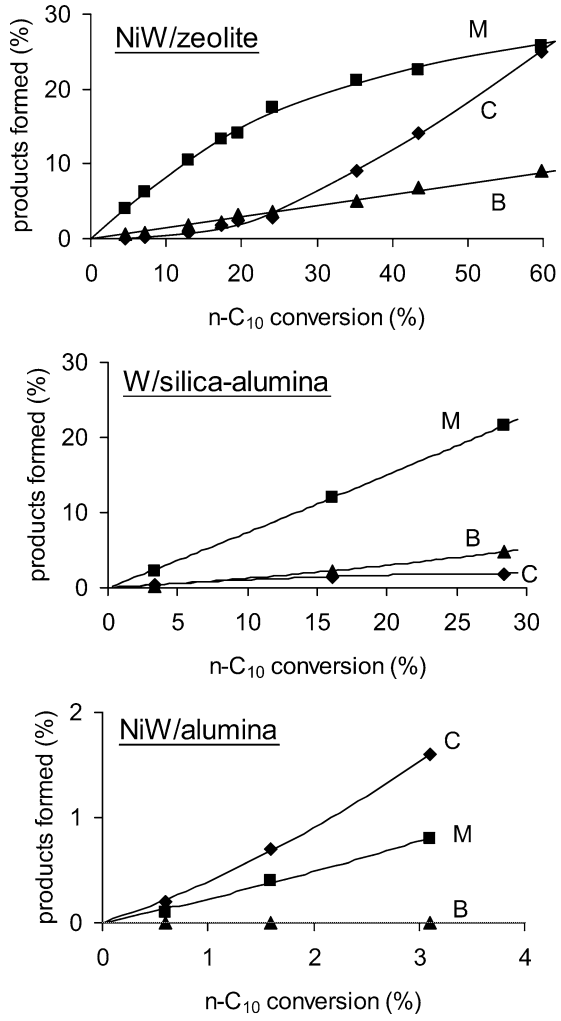

Fig. 7. Transformation of *n*-decane on NiW/zeolite, W/silica-alumina, and NiW/alumina: yields in the monobranched isomers M, in the multibranched isomers B, and in the cracking products C.

of conversions obtained. The M/B values measured with W/silica-alumina were smaller than those measured with NiW/silica-alumina and quite similar to those measured with NiW/zeolite (Fig. 8).

With NiW/alumina, the I/C ratio was about 0.5 in the range of conversions obtained (0.5–3%), the M/B ratio being infinite.

No significant difference was observed in the distribution of M or B products on all the catalysts (NiW/alumina excepted which produced no B products). On the contrary, differences existed in the distribution of the cracking products. Table 3 compares this distribution at low *n*-decane conversion (3–7%) or at high *n*-decane conversion (24–28%). In the case of NiW/alumina, the comparison was possible only at low conversion due to the weak activity of the catalyst. It can be seen that, at low conversion of *n*-decane, the distributions of the cracking products were very similar on NiW/silica-alumina, W/silica-alumina, and NiW/alumina, but very different from the distribution obtained on NiW/zeolite: on this latter catalyst, C_2 and C_8

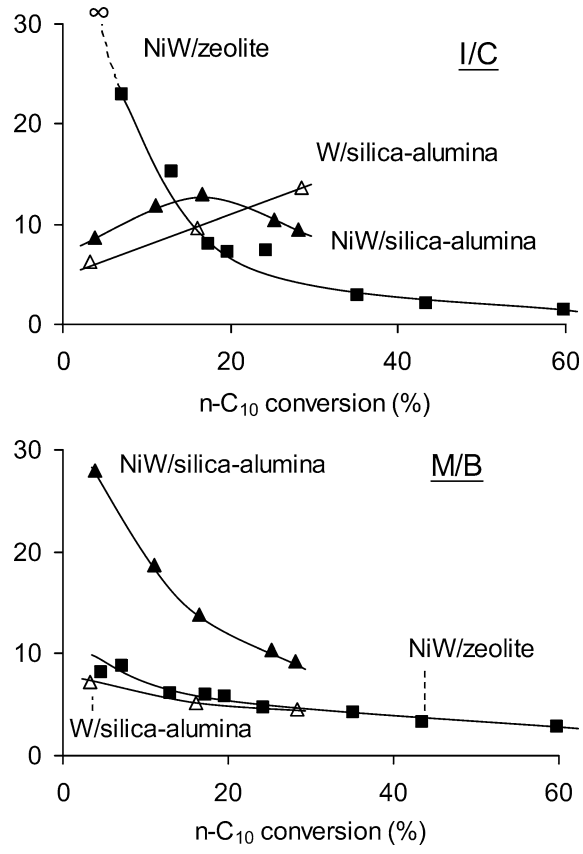

Fig. 8. Transformation of *n*-decane on NiW/silica-alumina, NiW/zeolite, and W/silica-alumina: isomerization/cracking ratio I/C and monobranched isomers/multibranched isomers ratio M/B. Isomerization and cracking values are wt%.

cracking products were practically not observed, while they were formed in significant amounts on the other catalysts. On the other hand, the branched products (iso) were much more favored on NiW/zeolite than on NiW/silica-alumina and W/silica-alumina, and especially on NiW/alumina. The distribution of the cracking products was not significantly modified on NiW/zeolite when the conversion of *n*-decane increased. On NiW/silica-alumina the amounts of C_2 and

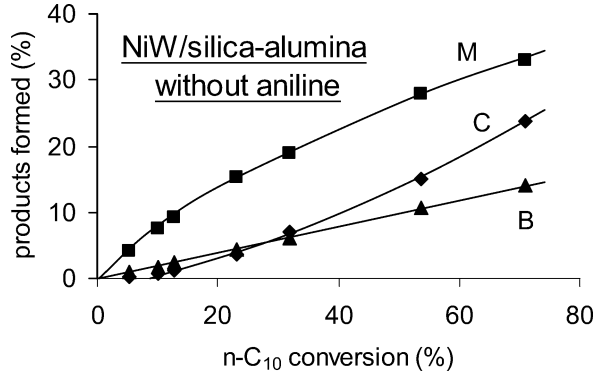

Fig. 9. Transformation of *n*-decane on NiW/silica-alumina in the absence of aniline: yields in the monobranched isomers M, in the multibranched isomers B, and in the cracking products C.

C_8 cracking products were smaller than at low *n*-decane conversion but always significant. On the opposite, C_2 and C_8 cracking products were barely observed on W/silica-alumina. The branched products were much more favored on NiW/zeolite, and also on W/silica-alumina, than on NiW/silica-alumina.

3.4. Hydrocracking of n-decane on NiW/silica-alumina in the absence of aniline

At the end of a standard experiment, the *n*-decane/dimethyl disulfide/aniline feed was simply replaced by a *n*-decane/dimethyl disulfide feed. The activity of NiW/silica-alumina began immediately to increase to reach a stable level after 4 h on stream. The activity of the catalyst in the absence of aniline was 225×10^{-4} mol h^{-1} g^{-1}, i.e., about 40 times higher than the activity in the presence of aniline, and 3 times higher than the activity of NiW/zeolite in the presence of aniline. Fig. 9 shows that, in the absence of aniline, the monobranched isomers M were always primary reaction products, but that the multibranched isomers B became also primary reaction products while the cracking products C became secondary reaction products, as evidenced in Fig. 10. This means that the reaction scheme

Table 3
Distribution (mol%) and iso/*n* ratios (mol%) of the cracking products formed on the various catalysts

	NiW/silica-alumina	W/silica-alumina	NiW/alumina	NiW/zeolite	NiW/silica-alumina	W/silica-alumina
X(*n*-C_{10})	4	3	3	7 or 24	28	28
C_2	18	18	12	1	9	3
C_3	14	14	19	9	15	12
C_4	15	14	18	26	21	24
C_5	14	15	15	31	20	25
C_6	12	13	15	25	17	24
C_7	22	21	14	8	13	11
C_8	5	5	7	0	5	1
iso/*n*-C_4	0.2	0.2	0	1.1	0.2	0.8
iso/*n*-C_5	0.2	0.3	0	1.5	0.2	1.1
iso/*n*-C_6	0.1	0.1	0.1	1.7	0.3	1.2
iso/*n*-C_7	0.2	0.1	0.1	2.3	0.4	1.2

X(*n*-C_{10}), *n*-decane conversion (%). When C_8 were observed, only *n*-C_8 was formed.

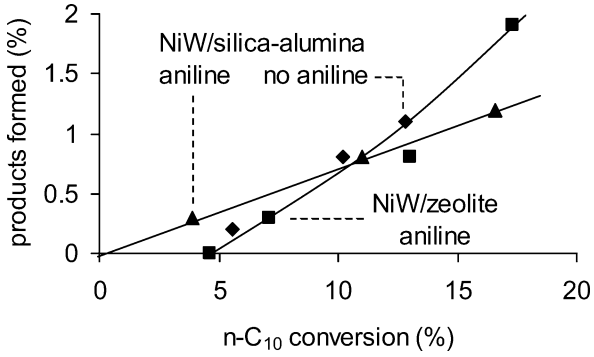

Fig. 10. Transformation of *n*-decane on NiW/silica-alumina in the presence or in the absence of aniline, and on NiW/zeolite in the presence of aniline: yields in the cracking products C.

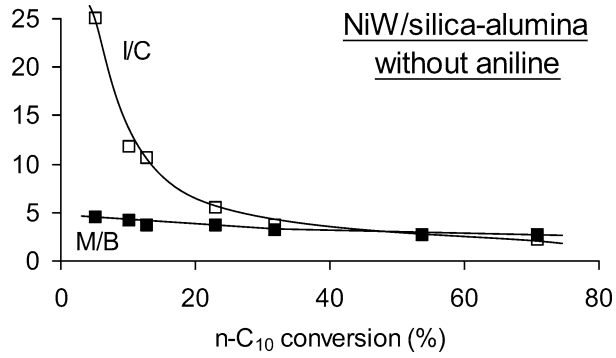

Fig. 11. Transformation of *n*-decane on NiW/silica-alumina in the absence of aniline: isomerization/cracking ratio I/C and monobranched isomers/multibranched isomers ratio M/B. Isomerization and cracking values are wt%.

is now similar to the one observed on NiW/zeolite in the presence of aniline (Figs. 7 and 10). This is confirmed by the fact that, at the same *n*-decane conversion, the I/C and the M/B ratios (Fig. 11) are very different from those measured in the presence of aniline (Fig. 3), and are similar to those measured on NiW/zeolite (Fig. 8). The absence of aniline did not modify the distribution of the monobranched isomers or that of the multibranched isomers which consequently remained similar to those observed on NiW/zeolite in the presence of aniline. The distribution of the cracking products and the iso/*n* ratio of these products were the same on NiW/silica-alumina in the absence of aniline as on NiW/zeolite in the presence of aniline, either at low or high conversion of *n*-decane (Table 4).

4. Discussion

Pyridine adsorption experiments clearly confirm that silica-alumina is much less acidic than the USHY zeolite, which is widely known. Compared to zeolite, silica-alumina has only few Brønsted acid sites. Moreover the strength of this sites is rather moderate, while a wide distribution in the acid strength is observed on zeolite. However, one can reasonably suppose that the strongest Brønsted acid sites of the

Table 4
Distribution (mol%) and iso/*n* ratios (mol%) of the cracking products formed on NiW/silica-alumina in the absence of aniline and on NiW/zeolite in the presence of aniline

	NiW/silica-alumina, no aniline,	NiW/zeolite, aniline,
$X(n\text{-}C_{10})$	5 or 23	7 or 24
C_2	1	1
C_3	10	9
C_4	26	26
C_5	30	31
C_6	25	25
C_7	8	8
C_8	0	0
iso/n-C_4	1.0	1.1
iso/n-C_5	1.3	1.5
iso/n-C_6	1.6	1.7
iso/n-C_7	2.4	2.3

$X(n\text{-}C_{10})$, *n*-decane conversion (%).

zeolite do not participate in *n*-decane hydrocracking because they are irreversibly poisoned by aniline or ammonia resulting from its decomposition.

The products of *n*-decane transformation on NiW/silica-alumina are those usually observed on classical hydrocracking catalysts such as NiW/zeolite, i.e., monobranched and multibranched isomers and cracking products. However, on NiW/silica-alumina the monobranched isomers and the cracking products are primary reaction products, and multibranched isomers are secondary reaction products, while on NiW/zeolite the monobranched and multibranched isomers are primary reaction products and cracking products are secondary reaction products.

On NiW/silica-alumina, the isomerization/cracking ratio (I/C) initially increases when the conversion of *n*-decane increases, which is again different from what is observed with NiW/zeolite on which I/C decreases regularly. This means that on NiW/silica-alumina cracking would be favored initially compared with isomerization, which suggests the existence of a direct cracking reaction of *n*-decane. This cracking produces significant amounts of C_2 and C_8 molecules which are not observed with bifunctional hydrocracking catalysts such as NiW/zeolite.

Isomerization superimposes on the direct cracking when the conversion of *n*-decane increases, which leads to an increase in the I/C ratio. Isomerization occurs most likely through a bifunctional mechanism since the distributions of the monobranched and of the multibranched isomers are the same as those observed on NiW/zeolite. At low *n*-decane conversion, the distributions of the isomers are different from the distribution at the thermodynamic equilibrium, which indicates that isomerization occurs through protonated cyclopropanes [17,18]. At high *n*-decane conversions the distributions tend toward those at the thermodynamic equilibrium, due to the appearance of alkyl shifts [19] which are more rapid than isomerization through protonated cyclopropanes [17].

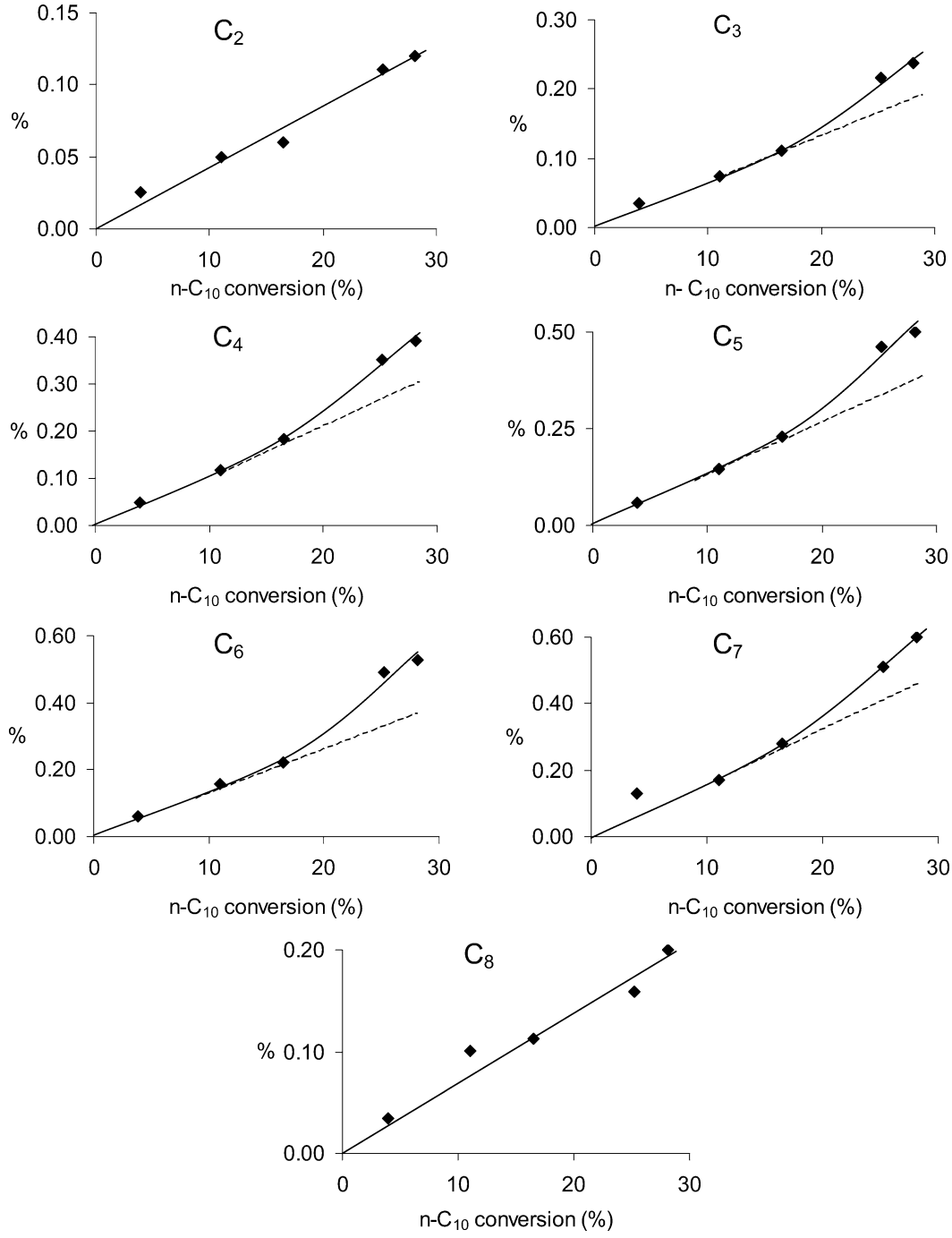

Fig. 12. Yields in the C_2–C_8 cracking products as a function of *n*-decane conversion.

The I/C ratio begins to decrease when the *n*-decane conversion becomes greater than 15–20%, which is due to an increase in cracking (Fig. 2). This is evidenced in Fig. 12 which shows the yields in the various cracking products as a function of *n*-decane conversion. The yields in all the cracking products increase linearly when the conversion of *n*-decane increases up to a 15–20% value. It must be noted that an anomalous high value is obtained for the C_7 yield at the lowest *n*-decane conversion, which is related with the high C_7 yield already shown in Fig. 4. The most likely explanation is the presence of traces of the sulfiding feed remaining in the unit, which would be observable only at low cracking levels. Above the 15–20% conversion value, the yields in C_2 and C_8 products always increase linearly, while the yields in the C_3–C_7 products increase more sharply. Therefore one can consider that the straight part of the curves represents only the direct cracking reaction. We also observed (Fig. 4) that the C_3/C_7 and C_4/C_6 molar ratios tend toward 1 when the conversion of *n*-decane increases. On bifunctional Pt/zeolite catalysts these ratios were always equal

to 1, whatever the conversion [20]. This suggests that the additional cracking observed at high *n*-decane conversion occurs through a bifunctional mechanism. However the direct cracking still exists since C_2 and C_8 continue to increase.

From the curves in Fig. 12, it is possible to estimate the relative importance of the direct cracking and of the bifunctional cracking: at a 28% *n*-decane conversion, the bifunctional cracking represents about 25% of the total cracking. It is also possible to estimate the amounts of the C_3–C_7 products resulting from the bifunctional cracking: C_3 and C_7 are formed in equimolar amounts, as well as C_4 and C_6. One can also calculate the bifunctional I/C ratio which is about 35, while the experimental I/C ratio (including the direct cracking) was only 10 (Fig. 8). This value is much higher than that measured with NiW/zeolite at the same conversion (about 5, Fig. 8). Lastly, it seems that the bifunctional cracking takes place mainly from the monobranched isomers. Indeed the cracked products are linear molecules in a large majority (the iso/*n* ratio of the cracked products is much smaller than 1). This is again different from what is observed with NiW/zeolite on which cracking occurs mainly from the more reactive multibranched isomers (iso/*n* ratio greater than 1). However the multibranched isomers are formed in small amounts on NiW/silica-alumina which makes their cracking products difficult to detect. An estimation of the iso/*n* ratio of the products formed through the bifunctional cracking is not possible since the direct cracking reaction can also concern the *n*-decane isomers.

Thus, the bifunctional transformation of *n*-decane on NiW/silica-alumina occurs through the step-by-step process shown in Scheme 1. Each olefinic intermediate formed from *n*-decane comes into contact with very few acid sites between two hydrogenating sites, and undergoes only one transformation, either branching or cracking [21], as evidenced by the high I/C (calculated) and M/B values. The acid step is clearly the rate-determining step of the bifunctional mechanism. This very weak acid activity is due to the adsorption on the acid sites of the ammonia produced through aniline decomposition.

On the other hand, in the absence of aniline all the acid sites are active, which allows one to find again on NiW/silica-alumina a classical bifunctional mechanism similar to the one observed with NiW/zeolite: rapid formation of the multibranched isomers, cracking occurring mainly from these latter (iso/*n* ratio greater than 1). Although the multibranched isomers appear as primary reaction products, they cannot be formed directly from *n*-decane

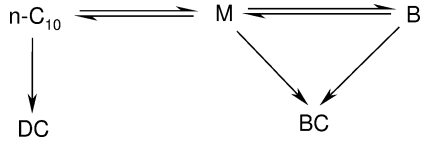

Scheme 1. Transformation of *n*-decane on NiW/silica-alumina: apparent reaction scheme. M, monobranched isomers; B, multibranched isomers; DC, direct cracking; BC, bifunctional cracking.

but only from the monobranched isomers. This means that the olefinic intermediates may encounter several acid sites during their diffusion between two hydrogenating sites [21]. However, they do not encounter enough acid sites to undergo cracking, the cracking products being always secondary reaction products.

The direct cracking reaction (DC) certainly does not occur through a bifunctional mechanism, since this would lead to the formation of unstable primary carbocations [22], nor through hydrogenolysis since methane is not observed [23]. On the other hand, this reaction is largely predominant on the nonacidic NiW/alumina catalyst, which indicates that it does not occur on silica-alumina but on the NiW sulfides. One can also note that this reaction is favored by the presence of Ni: at high *n*-decane conversion the unpromoted W/silica-alumina catalyst looks more like NiW/zeolite than like NiW/silica-alumina (Table 3).

Scheme 2 proposes a mechanism allowing an explanation of the direct cracking reaction. The example chosen leads to the formation of ethane and octane, but this mechanism can account for all the cracking products formed, but not for C_1 and C_9 which are effectively not observed. We use here a simplified representation of a catalytic center made of a sulfur vacancy associated to two W atoms and of an adjacent sulfur anion [24,25]. The first step would be the adsorption on the exposed W atom of an olefin formed through the dehydrogenation of *n*-decane on the hydro-dehydrogenating function of the catalyst. The second step would be the removal of a proton from the adsorbed olefin by the sulfur anion S^{2-} with the concomitant breaking of a C–C bond and formation of a C–W bond. This mechanism is quite similar to the one proposed to explain the breaking of the C–S bonds occurring during hydrodesulfurization reactions on sulfide catalysts [26]. In the present case it would lead to the desorption of an ethylene molecule further hydrogenated into ethane. Lastly, the breaking of the C–W bond allows the adsorbed olefin to recover its hydrogen atom and the catalytic site to recover its initial structure. The desorbed olefin finally hydrogenates into *n*-octane.

It must be noted that this mechanism does not involve carbocations at the difference of a classical bifunctional mechanism. It could also apply to the direct cracking of the monobranched isomers and of the multibranched isomers, unless the reaction would be slowed down too much by steric hindrance as is the case in hydrodesulfurization [27,28]. The last argument in favor of this mechanism is the fact that the direct cracking reaction is more significant on NiW/silica-alumina than on W/silica-alumina. Indeed, it is generally admitted that, on sulfide catalysts, the promoter decreases the strength of the metal-sulfur bonds in the sulfide [29] and increases the electronic density on the sulfur atoms [30], which can also be interpreted in terms of an enhancement of the basicity of these latter [31]. Thus, the removal of a proton from the molecule would be more rapid on the promoted catalyst than on the unpromoted one.

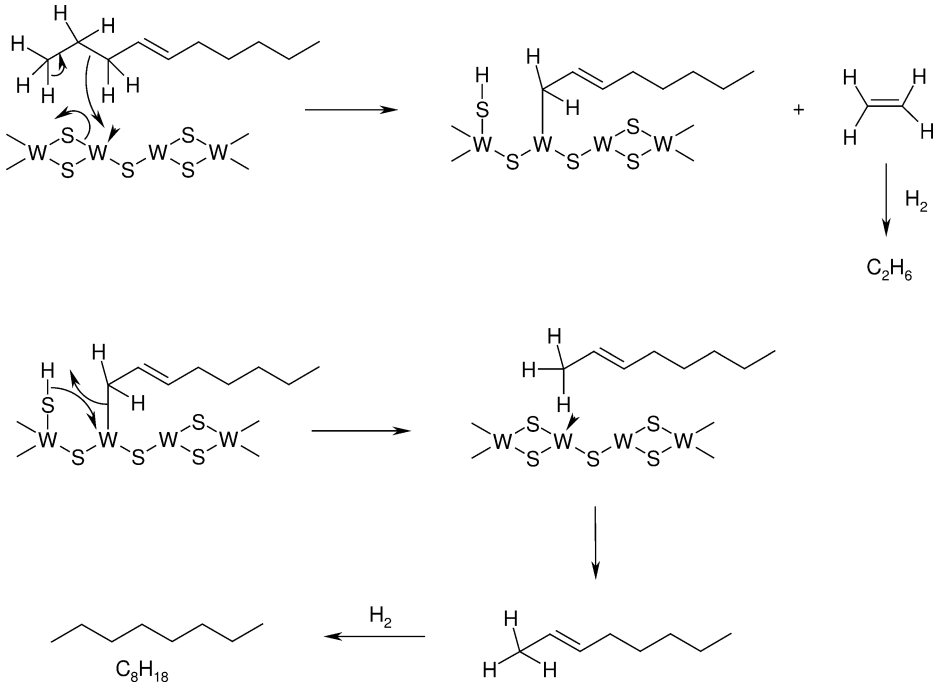

Scheme 2. Possible mechanism for the direct cracking of *n*-decane on the NiW sulfides.

5. Conclusion

The results obtained in the present work indicate that the behavior of the NiW/silica-alumina catalyst for *n*-decane hydrocracking in the presence of nitrogen-containing compounds is very different from that of classical hydrocracking catalysts such as NiW/USHY zeolite. The main reaction observed is the transformation of *n*-decane into monobranched isomers, the bifunctional transformation of which into multibranched isomers and into cracking products being hardly observed. On NiW/zeolite the multibranched isomers and the cracking products are formed rapidly. This difference is due to the fact that the acid sites of silica-alumina are strongly poisoned by the nitrogen-containing compounds present in the feed. In the absence of these compounds, all the acid sites of NiW/silica-alumina are active and the catalyst presents the same behavior as NiW/zeolite in the presence of nitrogen-containing compounds.

The little importance of the bifunctional cracking on NiW/silica-alumina allowed us to evidence the existence of a direct cracking of *n*-decane occurring not on the silica-alumina support but on the sulfide function of the catalyst. The mechanism proposed to explain this reaction involves the removal of a proton of the molecule by a basic sulfur atom. One can suppose that this reaction also occurs on the classical zeolite-sulfide catalysts, but that it is masked by the bifunctional cracking which is very fast due to the strong acid activity of the zeolite. In the case of NiW/silica-alumina, only high conversion levels would allow one to neglect this reaction.

The low cracking activity of the NiW/silica-alumina catalyst makes it very likely selective for the transformation of vacuum distillates into gas oil, which was the objective of this work. However, the global activity of the catalyst is rather low due to a too weak acidic function. It will be necessary to look for other supports, slightly more acidic than the silica-alumina used in the present work, in order to increase the global activity without appreciable change in the cracking activity.

References

[1] J.A.R. Van Veen, in: M. Guisnet, J.P. Gilson (Eds.), Zeolites for Cleaner Technologies, in: Catalytic Science Series, Vol. 3, Imperial College Press, London, 2002, p. 131.
[2] J. Sherzer, A.J. Gruia, Hydrocracking Science and Technology, Dekker, New York, 1996.
[3] J.W. Ward, Fuel Process. Technol. 35 (1993) 55.
[4] A. Corma, Catal. Lett. 22 (1993) 33.
[5] A. Hennico, A. Billon, P.H. Bigeard, J.P. Peries, Rev. Inst. Français Pétrol. 48 (1993) 127.
[6] P. Dufresne, P.H. Bigeard, A. Billon, Catal. Today 1 (1987) 367.
[7] Q. Chen, P. Van den Oosterkamp, S. Barendregt, Petrol. Technol. Q. 4 (1999) 47.
[8] J.K. Minderhoud, J.A.R. Van Veen, A.P. Hagan, Stud. Surf. Sci. Catal. 127 (1999) 3.
[9] I.E. Maxwell, Catal. Today 1 (1987) 385.
[10] A. Corma, A. Martinez, V. Martinez-Soria, J.B. Monton, J. Catal. 153 (1995) 25.
[11] M.A. Camblor, A. Corma, A. Martinez, V. Martinez-Soria, S. Valencia, J. Catal. 179 (1998) 537.
[12] A. Corma, A. Martinez, S. Pergher, S. Peratello, C. Perego, G. Bellusi, Appl. Catal. A 152 (1997) 107.
[13] S. Morin, P. Ayrault, N.S. Gnep, M. Guisnet, Appl. Catal. A 166 (1998) 281.
[14] W. Daniell, U. Schubert, R. Glöcker, A. Meyer, K. Noweck, H. Knözinger, Appl. Catal. A 196 (2000) 247.
[15] H. Knözinger, P. Ratnasamy, Catal. Rev.-Sci. Eng. 17 (1978) 31.

[16] D.R. Stull, E.F. Westrum, G.C. Sinke, The Chemical Thermodynamics of Organic Compounds, Wiley, New York, 1969.
[17] F. Chevalier, M. Guisnet, R. Maurel, in: G.C. Bond, P.B. Wells, F.C. Tompkins (Eds.), Proceedings of 6th International Congress of Catalysis, Vol. 1, The Chemical Society, London, 1977, p. 478.
[18] J. Weitkamp, Ind. Eng. Chem. Prod. Res. Dev. 21 (1982) 550.
[19] M.L. Poutsma, in: J.A. Rabo (Ed.), Zeolite Chemistry and Catalysis, in: ACS Monograph, Vol. 171, 1976, p. 437.
[20] F. Alvarez, F.R. Ribeiro, G. Pérot, C. Thomazeau, M. Guisnet, J. Catal. 162 (1996) 179.
[21] M. Guisnet, F. Alvarez, G. Gianetto, G. Pérot, Catal. Today 1 (1987) 415.
[22] J. Weitkamp, P. Martens, A. Jacobs, Appl. Catal. 8 (1983) 123.
[23] J.A. Martens, R. Parton, L. Uytterhoeven, A. Jacobs, Appl. Catal. 76-1 (1991) 95.
[24] S. Kasztelan, D. Guillaume, Ind. Eng. Chem. Res. 33 (1994) 203.
[25] F. Bataille, J.L. Lemberton, P. Michaud, G. Pérot, M. Vrinat, M. Lemaire, E. Schulz, M. Breysse, S. Kasztelan, J. Catal. 191 (2000) 409.
[26] J. Mijoin, G. Pérot, F. Bataille, J.L. Lemberton, M. Breysse, S. Kasztelan, Catal. Lett. 71 (2001) 139.
[27] D.R. Kilanowski, H. Teeuwen, V.H.J. de Beer, B.C. Gates, G.C.A. Schuit, H. Kwart, J. Catal. 55 (1978) 129.
[28] M. Houalla, D.H. Broderick, A.V. Sapre, N.K. Nag, V.H.J. de Beer, B.C. Gates, H. Kwart, J. Catal. 61 (1980) 523.
[29] H. Topsoe, B.S. Clausen, F.E. Massoth, in: J.R. Anderson, M. Boudard (Eds.), Catalysis, Science and Technology, Vol. 11, Springer, Berlin, 1996.
[30] H. Topsoe, B.S. Clausen, N.Y. Topsoe, E. Pedersen, W. Niemann, A. Müller, H. Bögge, B. Lengeler, J. Chem. Soc., Faraday Trans. I 83 (1987) 2157.
[31] J. Mijoin, V. Thévenin, N. Garcia Aguirre, H. Yuze, J. Wang, W.Z. Li, G. Pérot, J.L. Lemberton, Appl. Catal. A 180 (1999) 95.